ON THE FORCES AND STROUHAL NUMBERS IN THE LOW REYNOLDS NUMBER WAKES OF TWO CYLINDERS IN TANDEM

Tinghui Zheng[1], S. K. Tang[2], Baoling Fei[2]
[1] *Department of Applied Mechanics Sichuan University, China*
[2] *Department of Building Services Engineering, The Hong Kong Polytechnic University, Hong Kong, China*
E-mail: besktang@polyu.edu.hk

Received October 2007, Accepted September 2009
No. 07-CSME-49, E.I.C. Accession 3018

ABSTRACT

The flow around two circular cylinders of equal diameter in tandem arrangement was investigated numerically using the finite volume method in the present study. The code was validated by comparison with previous works at the Reynolds number of 200. A systematic investigation of the relationships of Strouhal number and the aerodynamic forces with cylinder separation and Reynolds number was done. Results demonstrate not only the important combined effects cylinder separation and Reynolds number on the wake aerodynamics, but also on the relative strengths of the forces acting on the two cylinders (both mean and fluctuations)

AU SUJET DES FORCES ET NOMBRES DE STROUHAL DANS LES TRAINÉES AÉRODYNAMIQUES AU BAS NOMBRES REYNOLDS DE DEUX CYLINDRES EN TANDEM

RÉSUMÉ

Dans cette étude, suivant la méthode des volumes limités, on a fait une recherche numérique du courant autour de deux cylindres circulaires, d'un diamètre identique et placés en tandem. Le code était validé par comparaison avec des études précédentes au nombre Reynolds de 200. On a examiné systématiquement les corrélations du nombre Strouhal et des forces aérodynamiques avec la séparation des cylindres et le nombre Reynolds. Les résultats démontrent les effets importants combinés du nombre Reynolds et de la séparation des cylindres sur les trainées aérodynamiques. Ils font aussi ressortir les effets sur les puissances comparées des forces agissant sur les deux cylindres (en moyenne et en fluctuation).

1. INTRODUCTION

Flows over two identical circular cylinders in tandem arrangement are found in many engineering applications. Groupings of transmission lines, bundles of tubes in heat exchangers, bridge piers and cables, pipelines and skyscrapers are some examples of these fundamental and challenging fluid mechanics problems.

The separated wakes from the two cylinders in tandem interact with each other and greatly complicate the flow dynamics. The cylinder separation to diameter ratio, L/D, where L is the center to center distance of the two cylinders and D the cylinder diameter, plays an important role in deciding the flow interference regime of such flow [1]. For small L/D, the shear layers separated from the upstream cylinder roll up behind the downstream cylinder. As L/D increases, the shear layers of the upstream cylinder will re-attach onto the downstream cylinder surface and only one vortex street exists behind the downstream cylinder. A transition from the re-attachment regime to the co-shedding regime occurs upon further increase in L/D. A vortex street is formed behind each cylinder and a critical L/D is observed after which the drag, lift and Strouhal number (St) will experience a large variation. There are also experimental efforts for the understanding of the complex flows behind cylinder pairs. For instance, Sumner et al. [2,3] and Igarashi [4] studied the various flow patterns behind the cylinders experimentally. However, most of the experiments in existing literature, except visualization, are associated with Reynolds numbers higher than 10^4.

Limited numerical investigations have been conducted. The previous works are focused on two dimensional flows at low Reynolds numbers. For instance, Li et al. [5] and Sharman et al. [6] investigated the flow at $Re = 100$; Meneghini et al. [7] and Slaouti and Stansby [8] conducted the investigation at $Re = 200$; Mittal et al. [9] examined the flow at $Re = 100$ and 1000; Jester and Kallinderies [10] studied the flow at $Re = 80$ and 1000; Mizushima and Suehiro [11] did the investigation at $Re = 60$ and 100. Recently, researchers start to investigate the three dimensional effects on flow around two cylinders. Carmo and Meneghim [12] did the simulation for Re ranges from 160 to 320 while Kondo et al. [13] performed the two dimensional and three dimensional simulations at $Re = 1000$. It is concluded that the two dimensional simulation underestimates the critical L/D. The three dimensional effect becomes more significant as the Re and L/D increases. It is also observed that the three dimensional effects are suppressed when the downstream cylinder is placed at a distance smaller than the critical L/D, such that the two- and three-dimensional simulations are almost identical throughout the Re range investigated.

Most of the numerical studies have made efforts to complement the experimental results, mainly with the view of validating their own numerical schemes for predicting such complex-geometry flows. Information on the St in the wake of two tandem cylinders at some Re and certain L/D are recorded. However, a relatively systematic investigation of the St and the aerodynamic forces of two tandem cylinders are, to the knowledge of the authors, not available. Also, there are seemingly discrepancies in the numerically simulated St in existing literature because of insufficient domain, insufficient number of cells and/or large time steps. The present study aims to provide a relatively systematic investigation of the St in the wake of two tandem cylinders and the related aerodynamic forces, covering a Re range from 100 to 1000 for $1 \leq L/D \leq 8$. A two dimensional simulation is adopted though the three dimensional effect may affect the accuracy of the predicted critical L/D as the latter is not expected to change the fundamental trends of the St and force variations with Re and L/D. It has also been shown in Papaioannou et al. [14] that, when the downstream cylinder is located at a distance smaller than the critical one, three dimensional effects are suppressed compared to the single-cylinder case and the flow wake

keeps a two-dimensional state (See also Carmo and Meneghini [12]). However, three-dimensionality in the flow becomes more important when the spacing exceeds the critical value. The current simulation provides a qualitative analysis on the force fluctuations and St under various cylinder separations, but might under-predict the exact value of the critical spacing.

2. GOVERNING EQUATIONS AND NUMERICAL METHODS

2.1. Governing Equations

A schematic of the flow configuration is shown in Fig. 1. The two circular cylinders with radius D are located at $(\pm L/2, 0)$. The spacing ratio is defined as L/D. The motion of an incompressible viscous flow is governed by the Navier-Stokes equation and the equation of continuity respectively:

$$\frac{\partial \mathbf{u}}{\partial t} + (\mathbf{u}\cdot\nabla)\mathbf{u} = -\nabla p + \frac{1}{Re}\nabla^2\mathbf{u} \tag{1}$$

and

$$\nabla\cdot\mathbf{u} = 0, \tag{2}$$

where $\mathbf{u} = (u,v)$ is the velocity, t the time and p the fluid pressure. The Reynolds number $Re = U_\infty D/\upsilon$, where υ represents the kinematic viscosity and U_∞ is the mean streamwise flow velocity at the inlet boundary of the computational domain. Periodical boundary conditions are adopted for the domain top and bottom boundaries. At outflow boundary, each quantity is linearly extrapolated from the inner region. The no-slip condition is imposed at the cylinder surfaces. The St is defined as $St = fU_\infty/D$, where f is the vortex shedding frequency as in common practice.

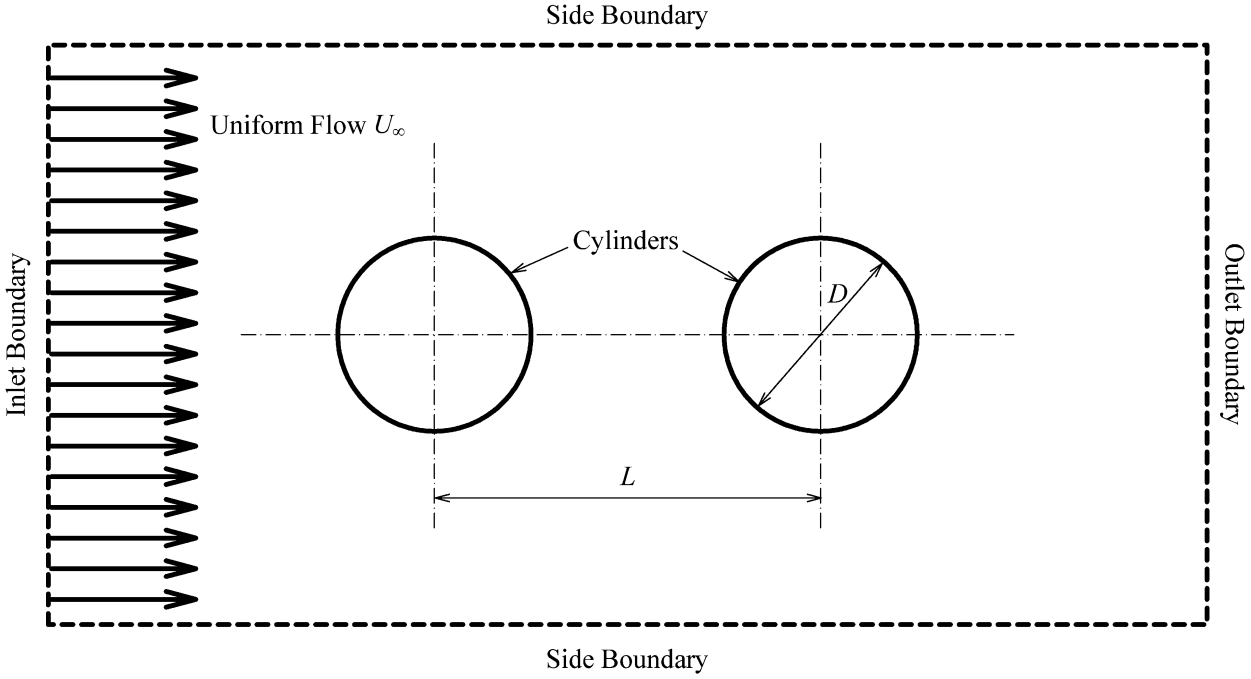

Fig. 1. Schematic for the tandem cylinder computational domain.

2.2. The Computational Method

A finite volume method was employed to solve the incompressible two dimensional Navier–Stokes equations. The multi-domain grid is used for dealing with the computations of flows along the two cylinders in tandem. Figure 2 shows the numerical grid generated using the GAMBIT grid generator where the O-grid is adopted around the cylinders and the Cartesian grids are adjacent to the O-grid. To resolve the near wall viscous region, the mesh around the cylindrical outer boundaries needs to be concentrated for better prediction of the wake dynamics. In the present study, a boundary layer with 10 rows is placed at the cylinder wall with the first cell height equal to $D/48$. All the related derivatives are discretized by the standard second-order centered difference scheme, but in order to minimize the numerical diffusion errors, QUICK scheme is used to approximate the advection terms. For the pressure interpolation at the cell faces, the PRESTO scheme was chosen because this scheme showed better results for cases where the pressure profile has a high gradient at the cell face [15]. The coupling between the pressure and velocity fields was done using the SIMPLE technique.

2.3. Domain Size Study

A domain independence study was implemented to ensure that the physics of the flow was modeled to within acceptable accuracy limits. The inlet boundary, side boundaries and outlet boundary were tested in turn with other boundaries kept fixed at the maximum level. The outcomes are summarized in Table 1. It is observed that the boundary distance plays an important role to the simulation results while the exit boundary distance affects the simulated flow patterns most significantly. Finally the inlet boundary was set at $10D$, the side boundaries were set at $15D$ and the exit boundary was set at $30D$ away from the cylinder array center respectively.

2.4. Grid Refinement Study

A grid refinement study was conducted for $L/D=4$. The computational domain is covered with three different meshes with grid spacing near the cylinder surfaces, ε, equals 0.0026, 0.002 and 0.0016 respectively. It is essential that the grid spacing at the cylinder surfaces has to be sufficiently small to resolve the velocity gradients in the boundary layers. The time variations of the lift coefficient C_l for the downstream cylinder obtained using the three meshes are shown in Fig. 3.

It can be concluded that the lift coefficient profiles for medium and fine numerical grids are almost the same. Therefore, the medium numerical grid was used in the following investigation. The time step is computed by $\Delta t U_\infty / D = C$, where C is taken to be 0.01, 0.02 and 0.04 respectively. It is found that the C_l profiles for $C = 0.01$ and 0.02 agree well with each other (not shown here). Thus, the Courant number is set as 0.02.

3. NUMERICAL RESULTS

3.1. Flow Patterns at $Re = 200$

In this section, the flows past two cylinders in tandem at Reynolds number 200 are studied in detail. The flow dynamics, the force coefficients and the vortex shedding frequency at different L/D are investigated. A comparison with the previous numerical results in existing literature is presented.

The present numerical study commences with the case of $L/D = 1$. It is expected that at this spacing ratio, the two cylinders will behave as one single flow obstacle and the vortex shedding

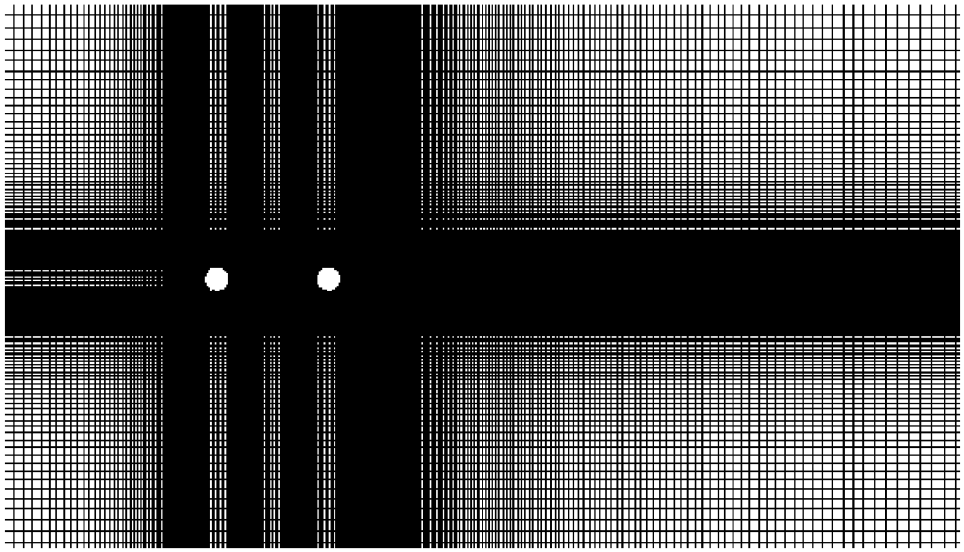

(a)

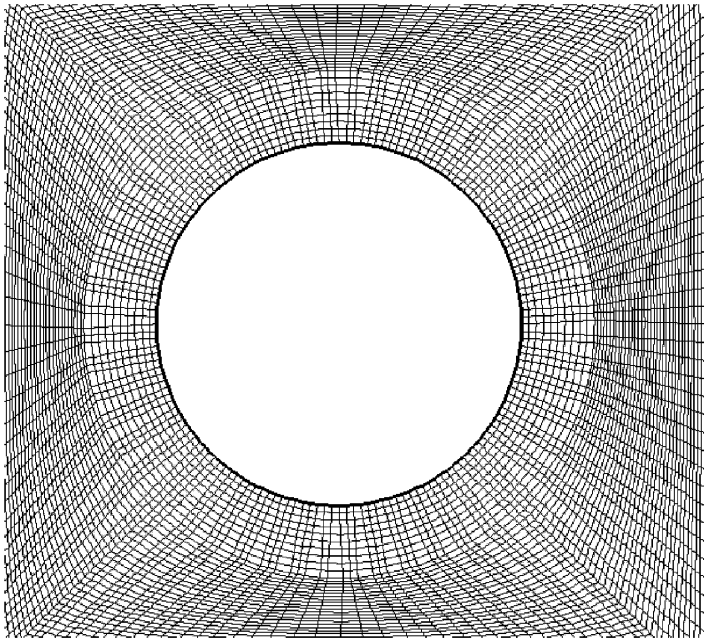

(b)

Fig. 2. The computational meshes. (a) Meshes arrangement for the whole domain; (b) meshes near the cylinder surface.

may be similar to that in the single cylinder case. However, there is no detailed investigation on its shedding frequency and the force coefficients. Figure 4a shows a typical set of instantaneous vorticity contours around two tandem cylinders with $L/D = 1$. The two tandem cylinder produces a longer shear layer compared with the single cylinder at the same Re (not shown here).

Typical sets of instantaneous vorticity contours for $L/D = 2$ and 4 are shown in Figs. 4b and 4c respectively. For $L/D = 2$, the shear layers separated from the upstream cylinder reattach onto the downstream cylinder. The vortex street only exists behind the downstream cylinder,

Table 1. The Comparison of the downstream cylinder Strouhal number for different domain size at Re=200 and L/D=4.0.

		Outlet boundary		
Inlet boundary (14D)	20D	25D	30D	35D
Side boundary (15D)	0.169	0.171	0.175	0.175
		side boundary		
Inlet boundary (14D)	8D	10D	15D	18D
outlet boundary (35D)	0.172	0.173	0.175	0.175
		inlet boundary		
outlet boundary (35D)	8D	10D	12D	14D
Side boundary (15D)	0.172	0.174	0.175	0.175

but the vortex length turns out to be very long. For $L/D = 4$, shear layers shed off from the upstream cylinder roll up into vortices before striking the downstream cylinder. Vortices are formed and shed from both cylinders. The major flow regimes found at low Re experimentally or numerically by other researchers (for instance, Meneghini et al. [7] and Zdravkovich [16]), namely ''single slender body'', ''reattachment'' and ''binary vortex streets'' are successfully recovered by the present code.

A comparison with the St results of other researchers is presented in Fig. 5. Results obtained using three-dimensional analysis [12,14] are also included for the sake of comparison. On the whole, the current simulation results have a good agreement with those in existing literature at similar Re except that of Slaouti and Stansby [8]. The experimental results of Igarashi [4], though were collected at $Re = 2.2 \times 10^4$, are included as reference. However, it is observed that the data of Igarashi [4] are basically inline with the present numerical results at $Re = 1000$ except at $L/D \sim 3$ probably because of the three-dimensionality effect which results in under-prediction of critical spacing by the two-dimensional numerical model at higher Re.

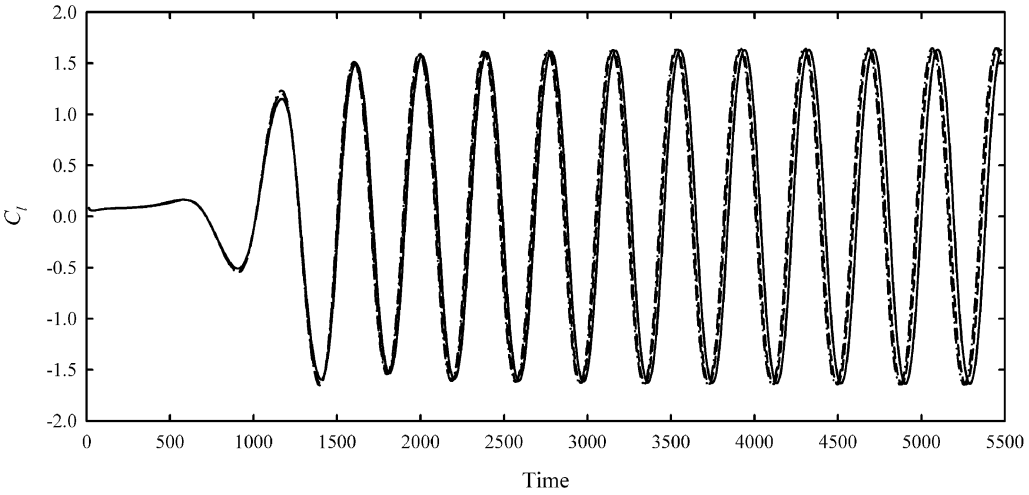

Fig. 3. Effects of near cylinder surface mesh sizes on the computations. —— : $\varepsilon = 0.0026$; − − − − − : $\varepsilon = 0.002$; — · — : $\varepsilon = 0.0016$.

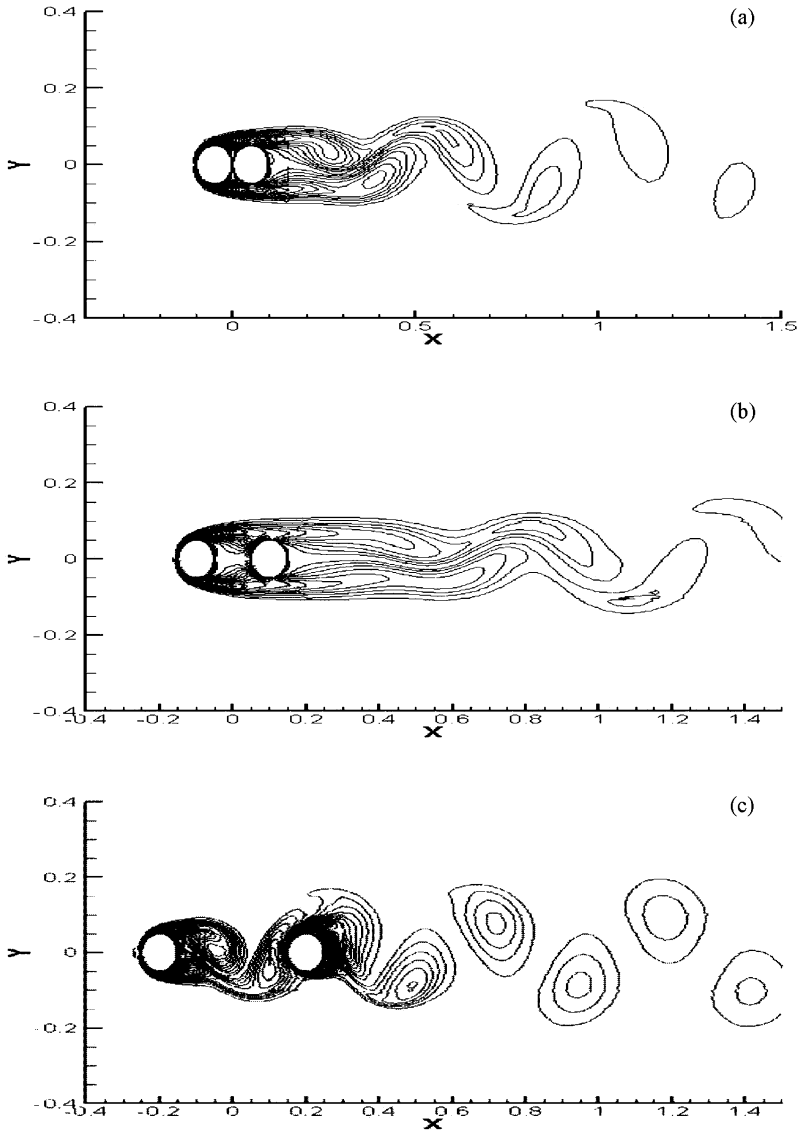

Fig. 4. Vorticity developments around the cylinders at $Re = 200$. (a) $L/D = 1$; (b) $L/D = 2$; (c) $L/D = 4$.

3.2. Dependence of *St* on *L*/*D* and *Re*

Figure 5 shows also the *St* as a function of L/D and *Re* ($100 \leq Re \leq 1000$). At $L/D = 1.5$, the shear layers originated from the upstream cylinder do not re-attach to the surface of the downstream cylinder for all *Re* tested and the *St* increases with *Re*. When L/D is increased to 2, the *St* drops because of the thickening of shear layers at this flow region [17]. The re-attachment of shear layer to the downstream cylinder allows the free shear layers to grow thicker before rolling up, resulting in a lower vortex shedding frequency and hence a decreasing *St*. For L/D ranging from 2 to 3 $\sim$ 4 and at low *Re*, the *St* increases very slowly which has also been observed by Sharman et al. [6]. In this region, the vortex shedding is still only observed behind the downstream cylinder. As the gap increases, the separation points of the cylinders move forward while the symmetrical flow pattern between the gap is disrupted as the L/D increases, resulting in the little increase of the *St*. For $Re \geq 500$, the *St* suddenly rises at $L/D \sim 2$. For *Re*

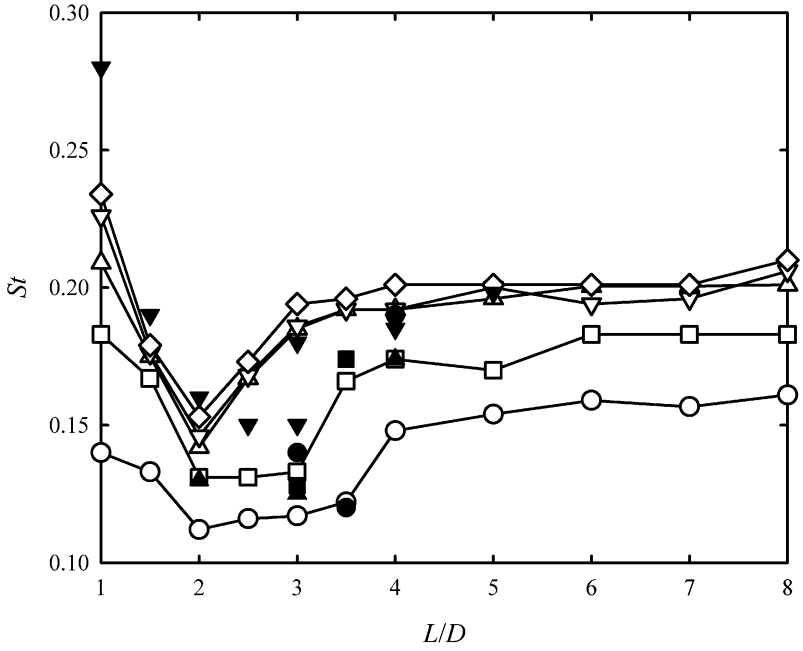

Fig. 5. Effects of *Re* and *L*/*D* on *St* in the cylinder wakes. ○ : *Re* = 100; □ : *Re* = 200; △ : *Re* = 500; ▽ : *Re* = 800; ◇ : *Re* = 1000; ● : Slaouti and Stansby [8]; ■ : Papaioannou et al. [13]; ▲ : Meneghini et al. [7]; ▼: Igarashi [4] ($Re = 2.2 \times 10^4$).

= 100, the critical *L*/*D* is ~4, while for *Re* = 1000, the value is 3. For *L*/*D* greater than the critical spacing ratio, the *St* rises slowly as the interaction between the cylinders is weakened. The *St* approaches that of a single cylinder as *L*/*D* becomes large. It is also observed that the minimum *St* at a fixed *L*/*D* decreases with decreasing *Re*.

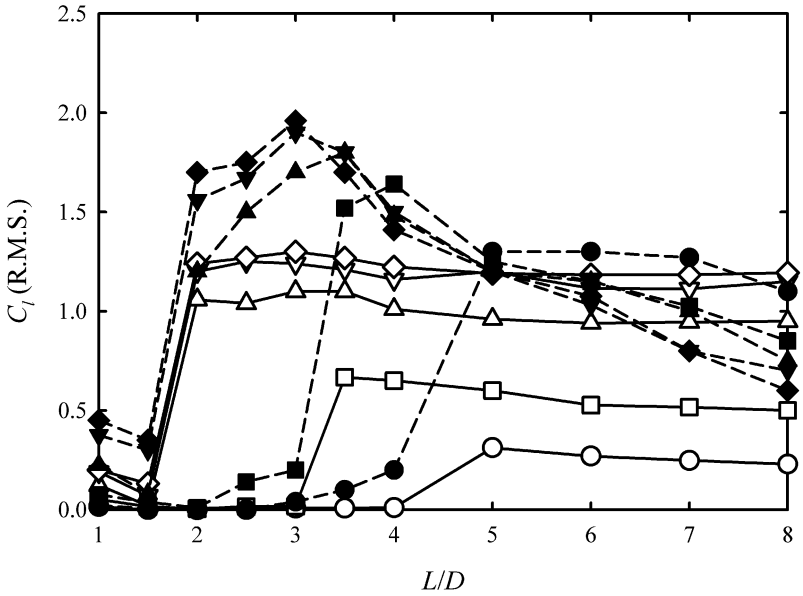

Fig. 6. Effects of *Re* and *L*/*D* on the C_l magnitudes. ○ : *Re* = 100; □ : *Re* = 200; △ : *Re* = 500; ▽ : *Re* = 800; ◇ : *Re* = 1000; open symbol : upstream cylinder; closed symbol : downstream cylinder.

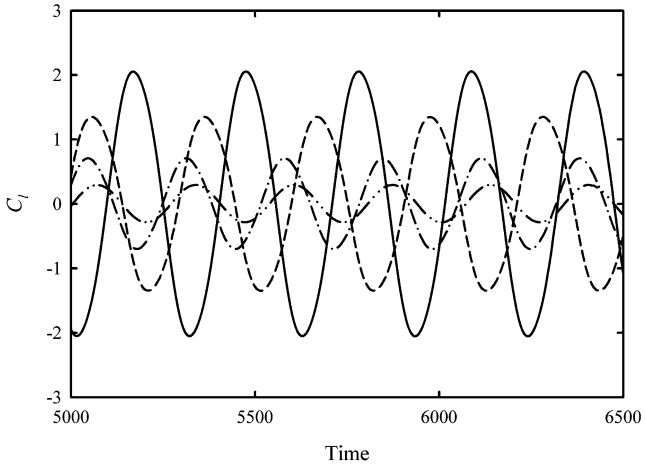

Fig. 7. Examples of lift fluctuations. —— : $Re = 500$, $L/D = 4$ (Downstream cylinder); − − − − − : $Re = 500$, $L/D = 4$ (Upstream cylinder); — · — : $Re = 1000$, $L/D = 1$ (Downstream cylinder); — · · — : $Re = 1000$, $L/D = 1$ (Upstream cylinder).

In general, the St increases with Re for all spacing ratio, but such increase slows down for $Re > 500$. Also, the variation of St with L/D does not change much when Re is increased beyond 500. In addition, one can notice that the range of L/D for the re-attachment regime is reduced as Reynolds number increases.

3.3. Variations of Drag and Lift with L/D and Re

Figure 6 illustrates the effects of L/D and Re on the magnitudes of the lift forces experienced by the two cylinders in term of the R.M.S. of the lift coefficient fluctuations. One can notice that the magnitude of the lift force acting on the upstream cylinder increases with the Re, but this is only true for the downstream cylinder at $L/D < 5$. Sharp rise of the C_ls for both cylinders is found within the re-attachment regime. In most of the cases, the lift force acting on the downstream cylinder is stronger than that on the upstream cylinder. Figure 7 shows some typical time fluctuations of C_ls. Owing to the sinusoidal nature of these fluctuations with negligible mean values, the R.M.S. values of the C_ls are proportional to their amplitudes.

Figure 8a shows that variations of the mean drag forces with Re and L/D. The C_d of the upstream cylinder varies only within a small range. However, that of the downstream cylinder goes from negative (pull towards the upstream cylinder) to positive (push away from upstream cylinder) with a sharp increase near the end of the re-attachment regime as L/D increases. Near the end of the re-attachment regime, the shear layers from the upstream cylinder hits the upstream side of the downstream cylinder resulting in the strong push mentioned. This push diminishes relatively quickly as L/D is increased further after the roll-up of the shear layers. The higher Re results in quicker the shear layer roll-up and thus faster decrease of the downstream cylinder C_d at the beginning of the isolated shedding regime. However, the mean drag of the downstream cylinder is also lower than that of the upstream one as expected.

The fluctuations of the downstream cylinder C_d are very strong compared to those happened to the upstream cylinder (R.M.S. values of C_d shown in Fig. 8b). The strengths of these fluctuations increase with Re. It can be concluded from Fig. 8 that the overall drag force acting on the upstream cylinder is always stronger that that acting on the downstream cylinder.

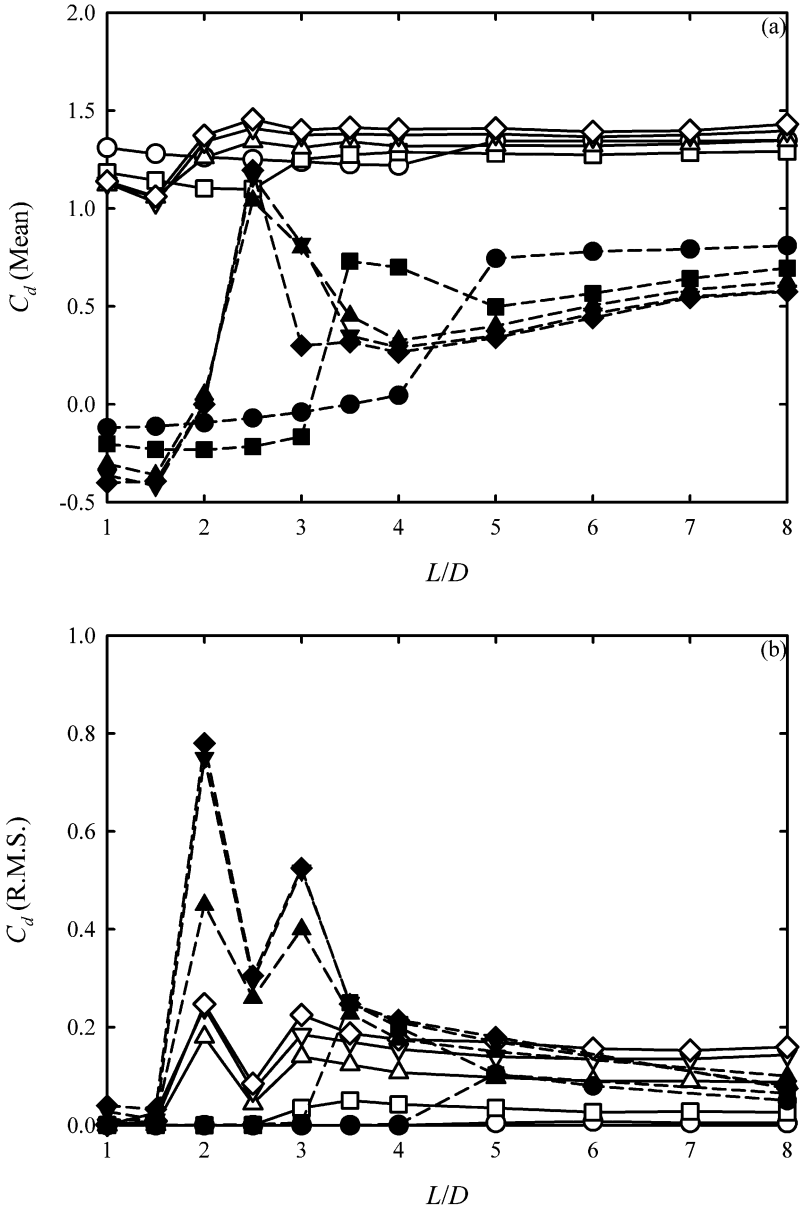

Fig. 8. Effects of *Re* and *L*/*D* on the C_d of the cylinders. (a) Mean C_d; (b) Root-mean-square of C_d fluctuation. Legends : same as those for Fig. 6.

4. CONCLUSIONS

The low Mach number flow dynamics and forces around two cylinders in tandem are numerically investigated in details in the present study. A systematic study on the relationships of the Strouhal number and the aerodynamic forces with the Reynolds number (up to 1000) and the cylinder separation gap (up to 8 cylinder diameters) is implemented. The computation code adopted was validated using data in existing literature at a Reynolds number of 200.

The Strouhal number increases with the Reynolds number, but the increase becomes not significant when the latter is increased beyond 500. The range of the gap to cylinder diameter

ratio for the occurrence of the re-attachment regime of the two tandem cylinder flow decreases as the Reynolds number increases.

It is found that the fluctuating lift force acting on the downstream cylinder is stronger than that on the upstream cylinder. An abrupt rise in the lift coefficient for both cylinders is observed within the re-attachment regime. Also, while the lift force acting on the upstream cylinder is stronger at higher Reynolds number, that on the downstream cylinder shows the opposite when the cylinder separation gap is larger than five diameter of the cylinder.

The drag force acting on the upstream cylinder does not vary much in the Reynolds number and gap distance ranges adopted in the present study. That acting on the downstream cylinder has larger fluctuations. Also, it changes from a pulling mode towards the upstream cylinder to a pushing mode as the cylinder separation increases. A substantial rise in this pushing drag force is always observed at the end of the re-attachment flow regime. However, the overall drag on the downstream cylinder is always weaker than that on the upstream cylinder, except at high Reynolds number and a particular cylinder separation where the two drags have similar magnitudes.

Since the cylinder flow will become turbulent under further increase in the Reynolds number and the three-dimensionality of the flow will become important, a change in the computational code will be necessary and this is left to further investigations.

ACKNOWLEDGMENTS

THZ's post-doctoral study in PolyU was supported by a grant from the Research Grant Council, the HKSAR Government (Project no. PolyU 5266/05E).

REFERENCES

1. Zdravkovich, M.M., "Review of Flow Interference between Two Circular Cylinders in Various Arrangements," *Trans. ASME: J. Fluids Engrg.*, Vol. 99, pp. 618–633, 1997.
2. Sumner, D., Price, D.J. and Païdoussis, M.P., "Flow-pattern Identification for Two Staggered Circular Cylinders in Cross-flow," *J. Fluid Mech.*, Vol. 411, pp. 263–303, 2000.
3. Sumner, D., Richards, M.D. and Akosile, O.O., "Two Staggered Circular Cylinders of Equal Diameter in Cross-flow," *J. Fluids Struct.*, Vol. 20, pp. 255–276, 2005.
4. Igarashi, T., "Characteristics of the Flow around Two Circular Cylinders arranged in Tandem," *Bull. J.S.M.E.*, Vol. B24, No. 188, pp. 323–331, 1981.
5. Li, J., Chambarel, A., Donneaud, M. and Martin, R., "Numerical Study of Laminar Flows past Two Cylinders in Tandem and Staggered Arrangements," *Int. J. Numer. Methods Fluids*, Vol. 19, pp. 155–170, 1991.
6. Sharman, B., Lien, F.S., Davidson, L. and Norberg, C., "Numerical Predictions of Low Reynolds Number Flows over Two Tandem Circular Cylinders," *Int. J. Numer. Methods Fluids*, Vol. 47, pp. 423–447, 2005.
7. Meneghini, J.R., Saltara, F., Siqueira, C.L.R. and Ferrari Jr, J.A., "Numerical Simulation of Flow Interference between Two Circular Cylinders in Tandem and Side-by-side Arrangements," *J. Fluids Struct.*, Vol. 15, pp. 327–350, 2001.
8. Slaouti, A. and Stansby, P.K., "Flow around Two Circular Cylinders by the Random Vortex Method," *J. Fluids Struct.*, Vol. 6, pp. 641–670, 1992.
9. Mittal, S., Kumar, V. and Raghuvanshi, A., "Unsteady Incompressible Flows past Two Cylinders in Tandem and Staggered Arrangements," *Int. J. Numer. Methods Fluids*, Vol. 25, pp. 1315–1344, 1997.

10. Jester, W. and Kallinderis, Y., "Numerical Study of Incompressible Flow about Fixed Cylinder Pairs," *J. Fluids Struct*., Vol. 17, pp. 561–577, 2003.
11. Mizushima, J. and Suehiro, N., "Instability and Transition of Flow past Two Tandem Circular Cylinders," *Phys. Fluids*, Vol. 17, pp. 104–107, 2005.
12. Carmo, B.S. and Meneghini, J.R., "Numerical Investigation of the Flow Around Two Circular Cylinders in Tandem," *J. Fluids Struct*., Vol. 22, pp. 979–988, 2006.
13. Kondo, N. and Matsukuma, D., "Numerical Simulation for Flow Around Two Circular Cylinders in Tandem," *Int. J. Comput. Fluid Dyn*., Vol. 19, pp. 277–288, 2005.
14. Papaioannou, G., Yue, D.K.P., Triantafyllou, M.S. and Karniadakis, G.E., "Three-dimensionality Effects in Flow around Two Tandem Cylinders," *J. Fluid Mech*., Vol. 558, pp. 387–413, 2006.
15. Sleiti, A. K. and Kapat, J. S., "Fluid Flow and Heat Transfer in Rotating Curved Duct at High Rotation and Density Ratios," *J. Turbomachinery*, Vol. 127, pp. 659–667, 2005.
16. Zdravkovich, M. M., "The Effects of Interference between Circular Cylinders in Cross Flow," *J. Fluids Struct*., Vol. 1, 239–261, 1987.
17. Xu, G. and Zhou, Y., "Strouhal Numbers in the Wake of Two Inline Cylinders," *Expts. Fluids*, Vol. 37, pp. 248–256, 2004.